Nonlinear Acoustic-Pressure Responses of Oxygen Droplet Flames Burning in Gaseous Hydrogen

Hong Jip Kim, Chae Hoon Sohn, Suk Ho Chung*†
Department of Mechanical and Aerospace Engineering, Seoul National University
Jong Soo Kim
Environment Research Center, Korea Institute of Science and Technology

A nonlinear acoustic instability of subcritical liquid-oxygen droplet flames burning in gaseous hydrogen environment are investigated numerically. Emphases are focused on the effects of finite-rate kinetics by employing a detailed hydrogen-oxygen chemistry and of the phase change of liquid oxygen. Results show that if nonlinear harmonic pressure oscillations are imposed, larger flame responses occur during the period that the pressure passes its temporal minimum, at which point flames are closer to extinction condition. Consequently, the flame response function, normalized during one cycle of pressure oscillation, increases nonlinearly with the amplitude of pressure perturbation. This nonlinear response behavior can be explained as a possible mechanism to produce the threshold phenomena for acoustic instability, often observed during rocket-engine tests.

Key Words: Acoustic Instability, Nonlinear Response, LOX/GH_2 Flame, Extinction, Threshold Phenomena

Nomenclature

A_i : Pre-exponential factor in ith reaction step
b_i : Temperature exponent in ith reaction step
D_j : Diffusion coefficient of jth species
E_i : Activation energy in ith reaction step
H : Normalized nonlinear amplification contribution as defined in Eq. (12)
h : Specific enthalpy of mixture
h_j : Specific enthalpy of jth species
κ_i : Reaction rate constant in ith reaction step
L : Latent heat of evaporation of liquid oxygen
$\overline{M}$: Averaged molecular weight of mixture
M_j : Molecular weight of jth species
m : Radial mass flux ($\equiv \rho u r^2$)
n_s : Number of species
p : Pressure
Q : Total heat-release-rate as defined in Eq. (11)
Q' : Heat-release rate per unit length
Q''' : Heat-release rate per unit volume
R : Gas constant
$\overline{R}$: Universal gas constant
r : Radial coordinate
$\tilde{r}_f$: Flame front stand-off ratio
T : Temperature
t : Time
u : Radial velocity
V_C : Correction velocity
V_j : Diffusion velocity of jth species
$\dot{w}_j$: Net production rate of jth species
X : Mole fraction
Y : Mass fraction

Greeks

Θ_j : Thermal diffusion ratio
θ : Phase difference
λ : Heat conductivity of mixture
ρ : Density

† First Author
* Corresponding Author,
E-mail : shchung@snu.ac.kr
TEL : +82-2-880-7114; **FAX** : +82-2-883-0179
Department of Mechanical and Aerospace Engineering Seoul National University, Seoul 151-742, Korea.
(Manuscript **Received** August 30, 2000; **Revised** January 26, 2001)

ϕ : Phase angle
ω : Acoustic frequency

Subscripts

a : Oscillation amplitude
B : Saturation state of liquid
f : Condition at flame
g : Gaseous state
l : Liquid state
m : Mean
s : Droplet surface
∞ : Ambience

1. Introduction

Acoustic instability occurs when pressure oscillations are amplified by thermal interaction with chemical reaction (Harrje and Reardon, 1972; Culick and Yang, 1995). Although this thermal interaction is an intrinsic process, acoustic instability is often coupled with system instability because the character of acoustic modes as well as acoustic-instability tendency are strongly dependent on design parameters, such as chamber geometry and fuel-feed system.

In some combustion devices such as a pulse combustor, acoustic instability is a preferred mode to enhance combustion and heat transfer. However, it is usually destructive to combustion systems, particularly to aeropropulsion systems. Continuing efforts to improve the specific impulse of propulsion systems make the system more vulnerable to acoustic instability. Present-day economic constraints limit conventional engineering practice in which a number of full-scale tests are conducted to suppress acoustic instability. Therefore, better understanding of physical amplification mechanism leading to acoustic instability is required.

Acoustic instabilities may arise from any nonlinear processes such as atomization, turbulent mixing, and combustion. Among these, combustion process is of primary interest because it is the source of thermal energy that can amplify and sustain acoustic oscillations. In particular, highly nonlinear nature associated with finite-rate chemical kinetics is capable of producing a strong amplification. The influences of finite-rate chemistry can be demonstrated from a recent gas turbine development. To reduce pollutant formation, premixed combustion is desirable instead of conventional nonpremixed combustion. The physical nature of rate control in premixed flames, instead of diffusion control in nonpremixed flames, strengthens the thermal coupling between combustion and acoustic oscillations. As a consequence, gas-turbine engines, which used to be stable, become vulnerable to acoustic instabilities.

Microscopic approaches to elucidate fundamental physical insight underlying acoustic instability have been performed by adopting various simplified flame configurations such as stagnation-point flow, counterflow, and spherical droplet flame. These flame configurations can be building blocks in the laminar flamelet model for turbulent nonpremixed combustion. Effects of chemical kinetics on the amplification mechanisms of acoustic instabilities have been investigated by employing many different levels of reaction models. Strahle (1975) analyzed the acoustic response of droplet combustion in the forward stagnation-point region, calculating unsteady combustion that produces the impedance of droplet-flame response to acoustic waves. The adopted reaction model was the Burke-Schumann limit with infinite-rate kinetics.

The effect of finite-rate kinetics on acoustic response assuming one-step overall reaction has been analyzed for strained diffusion flames by employing the activation-energy asymptotics (Kim and Williams, 1994). The results showed that the acoustic response of strained diffusion flame near extinction regime can lead to an order-of-magnitude increase in amplification contributions comparing with those near equilibrium regime because the nonlinearity of finite-rate chemistry is dominant near extinction. The combustion of subcritical liquid oxygen (LOX) droplet burning in stagnant gaseous hydrogen (GH_2) has also been analyzed (Sohn et al., 1996) to identify the phase change effect on amplification mechanisms. It has been shown that the gas-phase quasi-steadiness prevails from a droplet surface to a distance in the order of

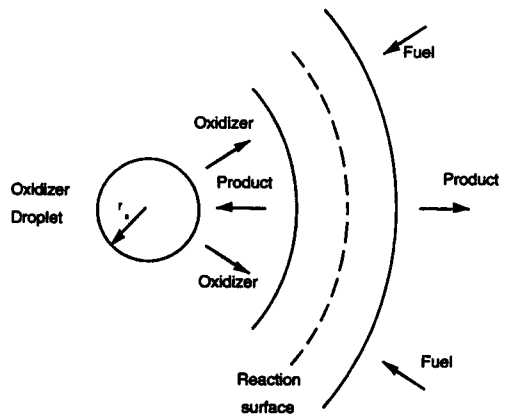

Fig. 1 Schematic of oxygen droplet combustion in gaseous hydrogen environment

$\sqrt{\rho_l/\rho_g}\, r_s \approx O(50) r_s$. Unlike hydrocarbon droplet flames burning in air, the chemical reaction zone of LOX droplet flames burning in gaseous hydrogen is located much closer to the droplet surface, so that the quasi-steadiness can be better justified in LOX-GH_2 flames. Immediately after the start-up period of rocket engines, the statistical property of droplet diameter distribution becomes stationary. Then, the analysis assuming gas-phase quasi-steadiness can be interpreted in the Eulerian sense, in which statistically identical droplet flames pass a fixed control volume. These asymptotic analyses (Kim and Williams, 1994; Sohn et al., 1996) with one-step overall reaction are restricted to linear stability considering a small amplitude of pressure oscillation.

As a further extension, the present study accounts the effects of detailed kinetic mechanism and of nonlinear behaviors of latent heat and saturation temperature with pressure during the phase change of oxygen. A 19-step detailed hydrogen-oxygen chemistry (Maas and Warnatz, 1988) replaces one-step overall chemistry used in the aforementioned analyses. By adopting numerical approach, nonlinear responses from a finite amplitude of pressure oscillation can be investigated.

2. Formulation

In order to simplify the problem, following approximations and assumptions are introduced. Since the characteristic time of droplet surface regression is larger than that of molecular diffusion of heat and mass by an order of ρ_l/ρ_g and the unsteadiness associated with droplet surface regression becomes significant in the far field approximately located $r/r_s \geq (\rho_l/\rho_g)^{1/2}$ (Crespo and Liñán, 1975), gas-phase quasi-steadiness compared to surface regression can be adopted. This assumption can be better justified for oxygen droplets with the flame front stand-off ratio much smaller than hydrocarbon droplets. Oxygen droplet flames burning in gaseous hydrogen, thus, exhibit a better quasi-steadiness in the near-field region where all the dominant processes including chemical reactions and transport phenomena take place. Consequently, droplet diameter can be considered to be instantaneously constant in the numerical calculation in the framework of diffusion-time scale. Although quasi-steadiness prevails in oxygen droplet flames, the resulting governing equations are treated as unsteady to account for pressure oscillations imposed on droplet burning.

By neglecting natural and forced convections, the analysis reduces to one-dimensional in the spherical coordinate. When droplet burning occurs at sufficiently subcritical pressure range, it has been found that the gas phase can be assumed ideal (Sohn et al., 1998). The phase change is at the equilibrium vaporization with pressure. Finally, the effect of viscous dissipation is neglected under low Mach number condition of droplet flames. The corresponding schematic diagram of droplet flames considered in the present analysis is shown in Fig. 1.

The conservation equations for the mass, momentum, energy and species, and the equation of state are as follows:

$$\frac{\partial \rho}{\partial t} + \frac{1}{r^2}\frac{\partial m}{\partial r} = 0 \tag{1}$$

$$p = p(t) = p_m + p_a \sin(2\pi\omega t) \tag{2}$$

$$\frac{\partial(\rho h)}{\partial t} + \frac{1}{r^2}\frac{\partial(mh)}{\partial r} - \frac{1}{r^2}\frac{\partial}{\partial r}\left(r^2\lambda\frac{\partial T}{\partial r}\right) + \frac{1}{r^2}\frac{\partial}{\partial r}\left(r^2\rho\sum_{j=1}^{ns} h_j Y_j V_j\right) - \frac{\partial p}{\partial t} = 0 \tag{3}$$

$$\frac{\partial(\rho Y_j)}{\partial t}+\frac{1}{r^2}\frac{\partial(mY_j)}{\partial r}+\frac{1}{r^2}\frac{\partial}{\partial r}(r^2\rho Y_jV_j)=w_jM_j \tag{4}$$

$$p=\frac{\rho\overline{R}T}{M} \tag{5}$$

where the radial mass flux m is deflned as $m\equiv\rho ur^2$ and p_m, p_a and ω are the mean pressure, the amplitude and frequency of pressure oscillations. The specifIc enthalpy of mixture h, the diffusional velocity V_j, and the average molecular weight of mixture $\overline{M}$ are

$$h=\sum_{j=1}^{ns}h_jY_j \tag{6}$$

$$V_j=-\frac{D_j}{X_j}\frac{\partial X_j}{\partial r}+\frac{D_j\Theta_j}{X_j}\frac{\partial(\ln T)}{\partial r}+V_c \tag{7}$$

$$\overline{M}=\left(\sum_{j=1}^{ns}Y_j/M_j\right) \tag{8}$$

Here, the Soret effect is included since the thermal diffusion of hydrogen molecule and radical are non-negligible in hydrogen-oxygen flames. The correction velocity V_c is included to ensure $\sum_{j=1}^{ns}Y_jV_j=0$. Thermodynamic and transport properties are calculated from the CHEMKIN-II (Kee et al., 1989) and the TRANSPORT package (Kee et al., 1983), respectively.

The hydrogen oxidation mechanism (Maas and Warnatz, 1988) is employed in this study, where the specific reaction-rate constant k_i of the ith reaction step is given in the Arrhenius form

$$k_i=A_iT^{bi}\exp(-E_i/RT) \tag{9}$$

The reaction rate of jth species, denoted by w_j, is the summation over all ith-steps involving jth species.

The boundary conditions are

$$\begin{aligned} r=r_s:\ &\lambda r_s^2\frac{\partial T}{\partial r}=mL \\ &T=T_{B,LOX} \\ &mY_j+\rho r_s^2Y_jV_j=m\delta(j-LOX) \end{aligned} \tag{10}$$

$$\begin{aligned} r\to\infty:\ &T\to T_\infty:\ \text{steady case} \\ &\rho\frac{\partial h}{\partial t}=\frac{\partial p}{\partial t}:\ \text{oscillation case} \\ &Y_j\to Y_{j,\infty}=\delta(j-GH_2) \end{aligned}$$

where the delta function is defined as $\delta(j-J)=1$ $(j=J)$ or 0 $(j\neq J)$.

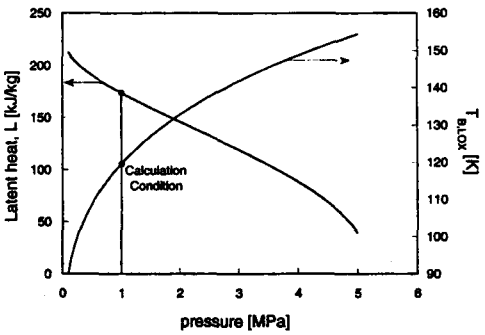

Fig. 2 Latent heat and saturated temperature of liquid oxygen as function of pressure

Variation of the saturation temperature, $T_{B,LOX}$, and the latent heat of LOX, L, with respect to pressure are shown in Fig. 2 (Sychev, 1987). As the pressure increases, the latent heat decreases moderately in the subcritical range of pressure.

Numerical calculations are performed based on the algorithm developed by Smooke (1982). A finite volume method is used to satisfy the convergence of independent variables at each node, and the Crank-Nicolson method and implicit method are optionally chosen for time integration. These are solved by using the modified Newton-iteration method, in which the computation time has been reduced by periodically calculating the Jacobian Matrix.

Steady-state characteristics of droplet flames are calculated at various pressures to obtain basic flame response. An inverse numerical method is employed, in which the flame structures are calculated as a function of maximum temperature instead of droplet diameter. Since flame structure is a single-valued function in the parameter space of maximum temperature, the inverse numerical method enables us to calculate flame structures beyond an extinction condition, where the conventional flame code fails to converge because of the high sensitivity of flame structure with respect to droplet diameter. This inverse numerical method provides flame structures near extinction with an improved accuracy, where flame responses to acoustic pressure oscillations are expected to be significant. Using the method, flame structures are also calculated as a function of pressure in order to demonstrate basic response behavior of flames

to pressure oscillations.

Special consideration has been taken in treating the boundary conditions at the far field. The profiles of temperature and species mass fractions decay algebraically, that is, decaying proportional to $1/r$. Such a slow convergence requires extremely large calculation domain to achieve sufficiently accurate far-field solutions. In order to circumvent this problem, the Dirichlet boundary conditions at infinity in Eq. (10) is replaced by weak boundary conditions, by applying asymptotic behavior at the far-field through convective-diffusive balance. By using this technique, sufficiently accurate solutions can be obtained with much reduced calculation domain size compared to the original problem, e. g., the domain of $r/r_s \leq 1000$.

3. Steady-State Flame Structure

Prior to analyzing the acoustic response of oxygen droplet flames to pressure oscillations, it is helpful to examine steady-state flame structures. Oxygen droplets injected in GH_2-LOX rocket engines have various diameters ranging from submicrometer to millimeter order. Since the characteristic diffusion time of droplets can be expressed as r_s^2/D, i.e., being proportional to the square of droplet diameter, the droplet combustion occurs in various chemistry regimes from near-equilibrium regime to near-extinction regime depending on droplet diameter (Law, 1975). The near-equilibrium regime is dominant for larger droplet flames, whereas the near-extinction regime is prevalent to droplet flames, whose droplet diameters are close to the extinction droplet diameter.

The resulting profiles of LOX droplet flame structures with various droplet diameters are obtained for $T_\infty=500$ K and $p_m=10$ atm, at which $T_{B,LOX}=119.63$ K and $L=173.6$ kJ/kg. The typical profiles of the temperature T and the heat-release rate per unit volume Q''' are shown in Fig. 3 for $r_s=1$ mm, which corresponds to the near-equilibrium condition.

For hydrogen diffusion flames, the flame structure is composed of a thin chain branching

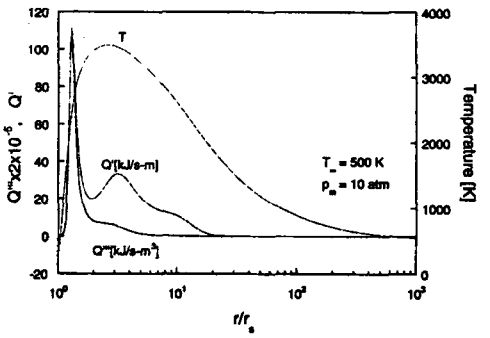

Fig. 3 The radial profiles of temperature T, heat-release rate per unit volume Q''' and heat-release rate per unit radial distance Q' for $r_s=1.0$ mm, $T_\infty=500$ K and $p_m=10$atm

zone embedded into a relatively broad recombination zone outside of which are non-reactive diffusive-convective zones for fuel and oxidizer transport (Chung and Williams, 1990). In the chain branching zone, the hydrogen-oxygen shuffle reactions of steps 1 to 4 are dominant. Thermal energy is mainly produced in the recombination zone (Lee et al., 1995). The dominant heat releasing steps in the recombination zone located on the oxidizer side of the chain-branching zone are (8) $H+O_2+M \leftrightarrow HO_2+M$ and (13) $HO_2+OH \leftrightarrow H_2O+O_2$. While the steps (5) $H+H+M \leftrightarrow H_2+M$ and (6) $H+OH+M \leftrightarrow H_2O+M$ are dominant in the fuel side due to the abundance of H-radical.

Examining the temperature and heat-release rate per unit volume in Fig. 3, two points are worthy of note. First, since the stoichiometric hydrogen to oxygen mass ratio is small, maximum temperature occurs at $r/r_s=2.6$. The parameter which determines the validity of gas-phase quasi-steadiness is the ratio of the liquid droplet density to the ambient gas density. For LOX droplet burning at 10 atm and $T_\infty=500$K, the liquid and ambient densities are $\rho_l=9.7506\times10^{-1}$g/cm^3 and $\rho_g=4.84927\times10^{-4}$g/cm^3, respectively. As mentioned previously, the gas-phase quasi-steadiness prevails for $r/r_s \leq \sqrt{\rho_l/\rho_g} \approx 45$, thus the quasi-steadiness can be justified for LOX-GH_2 droplet flames.

Secondly, Q''' shows somewhat different behavior compared with that of counterflow dif-

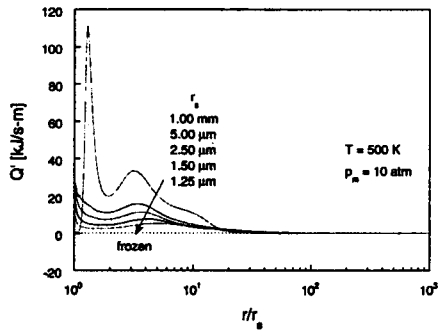

Fig. 4 Variations of heat-release rate per unit radial distance Q' in the radial coordinate for various values of the oxygen droplet radius

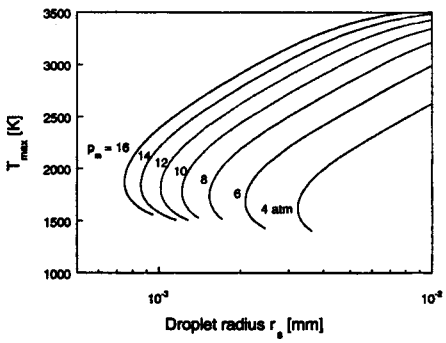

Fig. 5 Variations of maximum temperature with the droplet radius at various values of the mean pressure p_∞

fusion flames. For counterflow hydrogen-oxygen diffusion flames, it is predicted that two local maxima of heat-release rate exist on each side of the chain-branching zone (Lee et al., 1995). However, Q''' in the present study exhibits only one local maximum near $r/r_s=1.3$ in the oxidizer-side of the chain-branching zone. Since transport processes, thereby, heat release in droplet flames occurs in spherical symmetry, the heat-release rate per unit radial distance is defined as $Q'=4\pi r^2 Q'''$. The profile of Q' in Fig. 3 shows two local maxima corresponding to each side of the chain-branching zone. Therefore, the radical-recombination reactions exhibits similar contributions to total heat release as found in counterflow diffusion flames.

The profiles of Q' for various droplet radii are shown in Fig. 4. The characteristic diffusion time decreases with the square of the droplet radius, and so does the Damköhler number. The effect of finite-rate chemistry becomes operative for smaller droplet flames because of their shorter diffusion time. As a consequence, the peaks corresponding to the two local maxima of Q' for flames with a smaller droplet diameter become less distinguishable than those for flames with a larger droplet diameter and the peaks move closer to droplet surface, implying that there are significant leakage of the reactants, especially hydrogen, through the reaction zone. This is in conformity with the prediction of asymptotic analysis (Lee et al., 1995).

The overall steady-state behavior of oxygen droplet flames is shown in Figs. 5 and 6. Droplet diameter or pressure is obtained as an eigenvalue of the problem with a pre-specified maximum temperature using the inverse numerical method. Variations in the maximum flame temperature with various droplet sizes are plotted at several combustion-chamber pressure in Fig. 5. The extinction droplet diameter, corresponding to turning points, decreases with increasing chamber pressure, indicating that droplet flames at low pressures are easier to be extinguished.

Variations of the flame temperature with pressure, at various specified droplet diameters, are shown in Fig. 6. This plot is particularly useful in demonstrating the sensitivity of flame response with pressure, thereby could provide a qualitative description of the interaction mechanism of flame to pressure perturbation. Droplet flames with fixed droplet diameter can be extinguished by reducing ambient pressure, which can be identified by the turning points of the upper branch of S-shaped curves.

The magnitude of slope of maximum temperature with respect to pressure, which can be an indicator of flame sensitivity to pressure variation, increases as pressure decreases towards extinction pressure. This results for steady-state flame structure imply that the effect of finite-rate chemistry is more significant at low pressures. Also, the pressure-sensitivity suggests that the flame responses to acoustic oscillations are expected to be larger at low pressure and that a

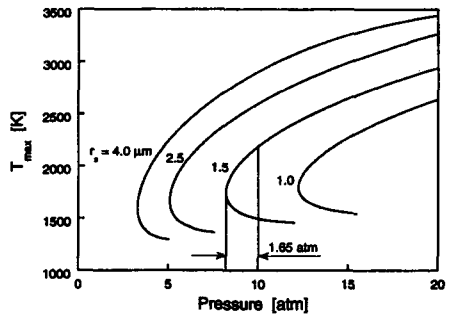

Fig. 6 Variations of maximum temperature with the mean pressure at various values of the oxygen droplet radius

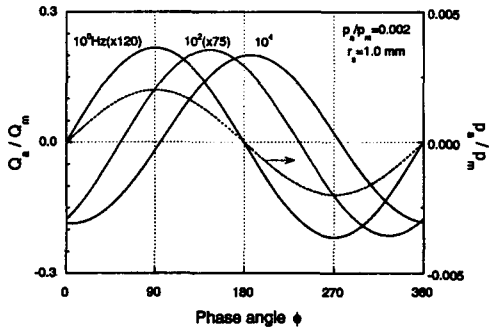

Fig. 7 Responses of total heat-release rate of a near-equilibrium flame for slow, medium and fast pressure oscillations

larger portion of the acoustic amplification contribution could arise when an acoustic pressure oscillation passes its minimum pressure.

4. Acoustic Response of Oxygen Droplet Flame

The contributions of droplet flames to acoustic instability can be judged by the Rayleigh criterion (Rayleigh, 1945). It states that acoustic amplification occurs if, on the average, heat is added in phase with pressure oscillation. The acoustic responses of oxygen droplet burning in gaseous hydrogen environment are examined for both near-equilibrium and near-extinction regimes.

It is to be noted that droplet flames may experience a substantial decrease in droplet diameter during pressure oscillations, although gas-phase unsteadiness does not play a major role in determining the flame structure as well as the flame response behavior. Therefore, the present results do not represent the acoustic response behavior of a single droplet in a Lagrangian sense, that is, in a moving coordinate attached to a droplet. Immediately after the start-up period of rocket engines, the statistical properties of droplet diameter distribution become stationary. Thus, the present results, obtained with constant droplet diameters, are to be interpreted in the Eulerian sense, in which statistically identical droplet flames pass a fixed control volume.

In order to understand the acoustic response of droplet flames, it is necessary to compare two characteristic times. One is the characteristic acoustic time, defined as the reciprocal of the acoustic frequency, and the other is the characteristic diffusion time of droplet flame. If a characteristic diffusion time is much shorter than a characteristic acoustic time, the flame tends to respond to pressure oscillations in a quasi-steady manner. In other words, the flame can rearrange its structure in a time scale comparable to the characteristic diffusion time. Then, the instantaneous flame structure should be very close to the quasi-steady flame structure corresponding to the instantaneous pressure. Consequently, the flame response would not exhibit any significant phase lag. In contrast, if a characteristic diffusion time is longer than a characteristic acoustic time, the flame could exhibit a noticeable phase lag with respect to pressure oscillation.

Corresponding to the imposed harmonic pressure variation given in Eq. (2), the acoustic response of a near-equilibrium droplet flame (r_s=1 mm) for various oscillation frequencies, namely a fast oscillation (10^4 Hz), an intermediate oscillation (10^2 Hz), and a slow oscillation (1 Hz), is shown in Fig. 7 as a function of the phase angle, ϕ. The response is represented in terms of Q_a/Q_m where Q is the total heat-release rate defined as

$$Q \equiv \int_{r_s}^{\infty} Q''' 4\pi r^2 dr = \int_{r_s}^{\infty} Q' dr \qquad (11)$$

where the subscript m denotes the steady-state

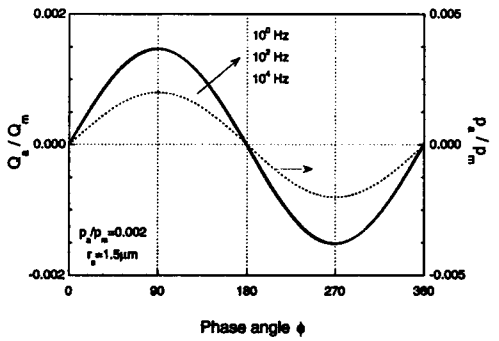

Fig. 8 Responses of total heat-release rate of a near-extinction flame for slow, medium and fast pressure oscillations

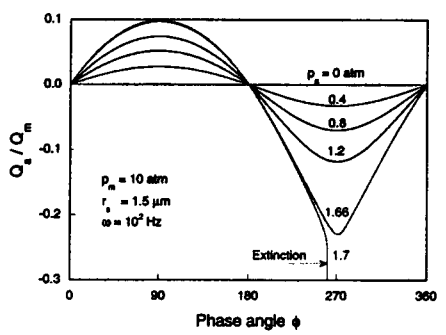

Fig. 9 Variations of the normalized heat-release responses for various amplitude of the pressure oscillation

corresponding to p_m and the subscript a denotes the acoustic part, i.e., the difference between the transient state and the steady state.

With increasing pressure, the latent heat of liquid oxygen decreases, thus the mass flux from a droplet surface to a reaction zone increases, resulting in an increase of the total heat-release rate Q. If the characteristic acoustic time is much longer(1 Hz) than the characteristic diffusion time, an increase(decrease) of the total heat-release rate Q occurs without having a noticeable phase lag with pressure increase(decrease), as seen from an excellent synchronization in Fig. 7. If the characteristic acoustic time is comparable or much shorter with the characteristic diffusion time, thermal energy is released with some phase delay with respect to pressure oscillation. Consequently, the cases of 10^2 Hz and 10^4 Hz show 50° and 95° delay, respectively. When phase lag occurs, the acoustic response will lead to an amplifying contribution only if the phase lag, normalized between ±180°, falls into the phase angle between −90° and +90° according to the Rayleigh criterion. Thus, 10^4 Hz oscillation could have an attenuation effect, while 1 Hz and 10^2 Hz have amplification effects.

The response of a flame in near-extinction regime (r_s=1.5 μm) is shown in Fig. 8. Since the characteristic diffusion time is much smaller than the acoustic time of both the fast and slow oscillation cases, the flame is capable of responding immediately to the pressure oscillations. Consequently, the fast, intermediate, and slow oscillation cases do not show any noticeable phase lag and exhibit almost identical response variations. This result implies that flames near extinction always have amplification effect, unless unrealistically high acoustic frequencies are imposed.

Acoustic responses to imposed pressure oscillation with various values of the pressure oscillation amplitude p_a are shown in Fig. 9 for ω=10^2 Hz, r_s=1.5μm, and p_m=10atm. Since the characteristic acoustic time is much longer than the characteristic diffusion time, no significant phase lags are observed, thereby exhibiting only the amplification contribution. When the pressure oscillations pass their minimum values, the droplet flames are closer to extinction. As a result, the fluctuations of the total heat-release rate, Q_a, are seen to be much greater near the phase angle of ϕ=270° compared to those of ϕ=90°, especially as p_a increases. In addition, the case of p_a= 1.7 atm shows that the flame can be extinguished if p_a is greater than a certain critical amplitude. The intensity of chemical reaction, especially in the near-extinction regime, is very sensitive to pressure variation. Thus, an excessive decrease of pressure leads to flame extinction.

For a near-extinction flame with p_m=10 atm and r_s=1.5μm, Fig. 10 shows the critical amplitude of pressure oscillations, p_a/p_m, as a function of acoustic frequency, above which flames are extinguished during pressure oscillation. When the acoustic frequency is low, the critical amplitude, p_a/p_m, is seen to be almost

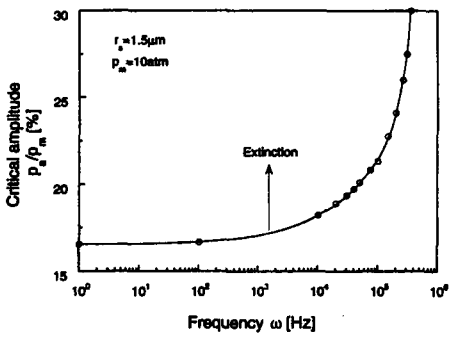

Fig. 10 Variations of the critical amplitude of the pressure oscillation to achieve flame extinction as a function of the acoustic frequency

invariant to acoustic frequency. However, as acoustic frequency increases, approximately above 10^3Hz, the critical amplitude of pressure oscillation increases rapidly. This can be caused by the unsteady effect which tends to impede flame's response to external pressure variation as frequency increases, thereby delaying flame extinction to a higher amplitude.

In order to evaluate the overall nonlinear amplification contributions of flames throughout one complete oscillation cycle, the heat-release-rate fluctuation is normalized in the form

$$H=\int_0^\tau [Q_a/Q_m]\sin(2\pi\omega t)dt \qquad (12)$$

According to the Poincaré-Lindstedt principle, as demonstrated by Culick (1963) for rocket engines and by Margolis (1993) for pulse combustors, the linear amplification rate can be defined as the slope of H times Q_m with respect to p_a at $p_a=0$, i.e., $Q_m[dH/dp_a]_{p_a}=0$. This type of the flame response function is ideal to apply to the acoustic-amplitude equation, which can be obtained by time-averaging the harmonically-decomposed conservation equations over an oscillation cycle. The variation of H with the normalized acoustic amplitude p_a/p_m is shown in Fig. 11 with the same conditions corresponding to Fig. 9.

The characteristics of the heat release response are seen to be quite nonlinear in that the increase of H with increasing p_a becomes greater as p_a becomes larger. The value of H is expected to become zero beyond the critical value of acoustic pressure amplitude $p_a=p_e$. Such response behavior can also be deduced from the steady flame structure shown in Fig. 6, in which greater nonlinear heat release response occurs when the instantaneous pressure passes near the minimum. As the acoustic amplitude increases, the flame becomes closer to extinction during the passage of the minimum pressure, so that the increase of H becomes greater. If p_a is greater than a critical value, which is 1.66atm in this calculation, then the chemical reaction during the passage of the minimum pressure is too weak to support the flame. Therefore, the flame is extinguished and the flame response vanishes.

The present results of nonlinear flame response can be viewed as a possible mechanism to produce the threshold phenomena discussed in the work of Clavin et al. (1994), in which acoustic instabilities can be triggered only by acoustic perturbations with amplitudes greater than a certain threshold amplitude. To show this possibility, three different damping response lines, each corresponding to strong, weak, and intermediate damping, are indicated in Fig. 11 by the dotted line, dashed line, and chain dotted line, respectively.

Although it is not essential, the damping lines are approximated by linear functions of pressure-oscillation amplitude. In principle, the amplification rate as well as the damping rate can be expressed by polynomial functions with odd powers. For many applications, a polynomial function with linear and cubic terms is sufficient to approximate damping rate. Since the nonlinearity associated with acoustic damping is generally much weaker than that of chemical reaction, the cubic nonlinear term in damping rate is expected to be effective much later than the nonlinear effects from finite-rate chemistry. Therefore, the damping rate is approximated as a linear function. The stationary amplitude of acoustic pressure oscillation can be found from the intersection of the amplification and damping lines, at which the effects of damping and amplification can balance each other.

First, consider the case of strong damping which is marked stable in Fig. 11. The only

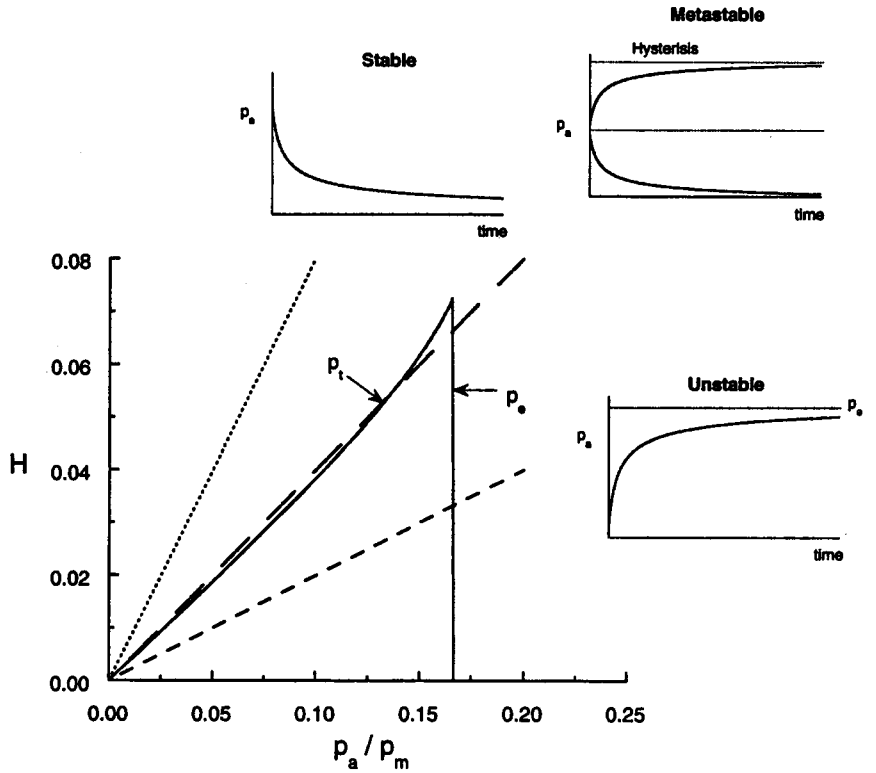

Fig. 11 Variations of the nonlinear heat-release response with normalized acoustic-pressure amplitude for $r_s=1.5\mu$m, $\omega=10^2$Hz and $p_m=10$ atm. Interaction with intermediate damping exhibits metastable characteristics

intersection between the amplification and damping rates occurs at $p_a=0$. This implies that any acoustic perturbation is attenuated and the system is stable. For the case of weak damping, there are intersections at $p_a=0$ and at $p_a=p_e$, and only the intersection at $p_a=p_e$ is stable. Therefore, all acoustic disturbance will eventually converge to $p_a=p_e$, and the system is always unstable. The third case corresponds to the intermediate damping, in which two stable intersections at $p_a=0$ and $p_a=p_e$ are separated by an unstable one at $p_a=p_t$. If the initial amplitude of a disturbance is greater than p_t, the acoustic amplitude converges to p_e. Otherwise, the disturbances are attenuated. Consequently, the system is meta-stable and exhibits threshold behavior.

Clavin et al. (1994) have demonstrated that such a meta-stable acoustic system can exhibit a bimodal distribution for the amplitude of acoustic waves. It is also worthy of note that, though the nonlinear response shown in Fig. 11 is calculated from a droplet-flame model, such response behaviors are expected from any type of flame configurations exhibiting high sensitivity near extinction.

5. Concluding Remarks

The structures and nonlinear acoustic-pressure responses of subcritical liquid-oxygen droplet flames burning in heated gaseous-hydrogen have been numerically studied by employing a detailed hydrogen-oxygen chemistry. The results of the quasi-steady flame structure analysis show that the droplet fames can be extinguished by reducing the chamber pressure sufficiently. The response sensitivity of flames to pressure perturbations,

measured in terms of the slope of the maximum temperature with respect to pressure, increases as pressure decreases toward an extinction pressure.

The nonlinear responses are examined by imposing harmonic pressure perturbations with various amplitudes on droplet flames in both the near-equilibrium and near-extinction regimes. The heat release for near-extinction LOX droplet flame always responded to pressure oscillations without noticeable delay, since the characteristic diffusion time of near-extinction droplet flame is much shorter than the typical value of characteristic acoustic time. In addition, a larger flame response occurs during the passage of minimum pressure because flames near extinction are more sensitive to pressure fluctuations. Consequently, the flame response, normalized during one complete oscillation cycle, increases with much faster rate than the rate of increase in the amplitude of pressure oscillation. This nonlinear response behavior can be interpreted as a possible mechanism in generating the threshold phenomena observed during rocket-engine tests.

Acknowledgement

Supports of this research were provided as follow : HJK, CHS and SHC by the Turbo and Power Machinery Research Center at Seoul National University, and JSK by the Korean Ministry of Science and Technology through Grant No. 2N15900 and by the U.S. Air Force Office of Scientific Research through AFOSR Grant No. F49620-94-1-0166. The authors also would like to thank Prof. F.A. Williams for many helpful discussions.

References

Chung, S.H. and Williams, F.A. , 1990, "Asymptotic Structure and Extinction of CO-H_2 Diffusion Flames with Reduced Kinetic Mechanisms," *Combustion and Flame*, Vol. 82, pp. 389~410.

Clavin P., Kim, J.S. and Williams, F.A., 1994, "Turbulence-Induced Noise Effects on High-Frequency Combustion Instabilities," Combustion Science and Technology, Vol. 96, pp. 61~84.

Crespo, A. and Liñán, A., 1975, "Unsteady Effects in Droplet Evaporation and Combustion," Combustion Science and Technology, Vol. 11, pp. 9~18.

Culick, F.E.C., 1963, "High-Pressure Oscillations in Liquid Rockets," *AIAA Journal*, Vol. 1, No. 5, pp. 1097~1104.

Culick, F.E.C., and Yang, V., 1995, "Overview of Combustion Instabilities in Liquid Propellant Rocket Engine," *Liquid Propellant Rocket Combustion Instability*, Vol. 169 of Progress in Astronautics and Aeronautics, edited by V. Yang, and W.E. Anderson, AIAA, Washington DC, pp. 3~38.

Harrje, D.J., and Reardon, F.H., Eds., 1972, *Liquid Propellant Rocket Instability*, NASA SP-194, NASA, Washington DC.

Kee, R.J., Warnatz, J. and Miller, J.A., 1983, "A Fortran Computer Code Package for the Evaluation of Gas-Phase Viscosities, Conductivities, and Diffusion Coefficients," *Sandia National Laboratories Report*, SAND83-8209.

Kee, R.J., Rupley, F.M. and Miller, J.A., 1989, "CHEMKIN-II : A Fortran Chemical Kinetics Package for the Analysis of Gas-Phase Chemical Kinetics," *Sandia National Laboratories Report*, SAND89-8009.

Kim, J.S., and Williams, F.A., 1994, "Contribution of Strained Diffusion Flames to Acoustic Pressure Response," Combustion and Flame, Vol. 98, No. 3, pp. 279~299.

Law, C.K., 1975, "Asymptotic Theory for Ignition and Extinction in Droplet Burning," Combustion and Flame, Vol. 24, pp. 89~98.

Lee, S.R., Park, S.S. and Chung, S.H., 1995, "Flame Structure and Thermal NO_x Formation in Hydrogen Diffusion Flames with Reduced Kinetic Mechanisms," *KSME International Journal*, Vol. 9, pp. 377~384.

Maas, U., and Warnatz, J., 1988, "Ignition Processes in Hydrogen-Oxygen Mixtures," *Combustion and Flame*, Vol. 74, pp. 53~69.

Margolis, S. B., 1993, "Nonlinear Stability of Combustion-Driven Acoustic Oscillations in Resonance Tubes," *Journal of Fluid Mechanics*,

Vol. 253, pp. 67~84.

Rayleigh, J. W. S., 1945, *The Theory of Sound*, Dover, New York, Vol. 2, pp. 226~235.

Smooke, M.D., 1982, "Solution of Burner Stabilized Premixed Laminar Flames by Boundary Value Methods," Journal of Computational Physics, Vol. 48, pp. 72~105.

Sohn, C.H., Chung, S.H., Kim, J.S. and Williams, F.A., 1996, "Acoustic Response of Droplet Flames to Pressure Oscillations," *AIAA Journal*, Vol. 34, pp. 1847~1854.

Sohn, C.H., Chung, S.H., Lee, S.R. and Kim, J. S., 1998, "Structure and Acoustic-Pressure Response of Hydrogen-Oxygen Diffusion Flames at High Pressure," *Combustion and Flame*, Vol. 115, pp. 299~312.

Strahle, W.C., 1965, "Periodic Solutions to a Convective Droplet Burning Problem: Stagnation Point," *10th Symposium (International) on Combustion*, The Combustion Institute, Pittsburgh, PA, pp. 1315~1325.

Sychev, V.V., 1987, *Thermodynamic Properties of Oxygen*, Hemisphere Publishing Corporation.

Tarifa, C. S., Crespo, A., and Fraga, E., 1972, "A Theoretical Model for the Combustion of Droplets in Super-critical Conditions and Gas Pockets," *Acta Astronautica* Vol. 17, pp. 685~692.